Catalysis Today 157 (2010) 223–230

Contents lists available at ScienceDirect

Catalysis Today

journal homepage: www.elsevier.com/locate/cattod

Do synthetic Fe-zeolites mimic biological Fe-porphyrins in reactions with nitric oxide?

Mickaël Rivallan*, Bryan Bromley, Lioubov Kiwi-Minsker

Ecole Polytechnique Fédérale de Lausanne (EPFL), GGRC-ISIC, Station 6, CH-1015 Lausanne, Switzerland

ARTICLE INFO

Article history:
Available online 13 May 2010

Keywords:
Fe–ZSM-5
Fe(Porph)
Nitric oxide
Alpha oxygen
Bent/linear nitrosyl

ABSTRACT

Iron containing ZSM-5 zeolites is extremely active in nitrous oxide decomposition. This reaction involves atomic oxygen species known as “alpha oxygen” on iron sites. Despite the multiple techniques devoted to its characterization, the active sites’ structure remains nevertheless unknown. Herein, these centers are quantified via surface titration by nitrous oxide followed by temperature programmed desorption and characterized via nitric oxide probe molecule followed by infrared spectroscopy. In this latter case, two mono-nitrosyl species differing in the bonds’ geometry are observed on the iron centers. Moreover, upon NO evacuation, the two corresponding IR bands suddenly transit to lower wavenumbers. A mirror trend is also reported in biology when NO interacts with iron porphyrins and explained in terms of linear to bent Fe–N–O modification. This structural change is reversible upon addition/evacuation of NO. In the present report, the same reversible nitrosyl transition is observed for Fe–ZSM-5. Based on the close analogies found, the active site’s structure in Fe–ZSM-5 is built-up from the porphyrinatoiron(II) model.

1. Introduction

Although natural porphyrin complexes are essential for life, synthetic porphyrins and their complexes have limited utility. Bio-inspired catalysts are under development mimicking the biological metal porphyrin centers. Powerful concept to translate the principles of enzymatic to non-biological catalysis remains a dream of many who works on nanostructured porous materials. Zeolites could be assumed as the ideal materials for such enzymatic-like catalysts, first because of the uniform pore-size distribution, rendering a material with extraordinary molecular discrimination abilities known as shape-selectivity, and also because this crystalline matrix is able to stabilize particular metal ions, reported as active sites for important oxidation reactions. For instance, Fe–ZSM-5 after thermal activation is found to be extremely active and selective in benzene and methane oxidation by N_2O at low temperature. These reactions have been shown to involve Fe(II)-sites forming atomic oxygen species known as “alpha oxygen” [1]. Despite the numerous papers and techniques devoted to its characterization, the structure of Fe active sites remains still debating. The main reason for this is that in spite of high activity, the Fe centers involved in such oxidation catalysis are present in very low concentration. As a consequence, their characterization becomes difficult. The main debating point concerns the nuclearity of Fe hosting site [2]. Dinuclear [3–9] and/or mononuclear [10–15] site(s) are the most proposed and expected structures, where an Al atom(s) remain(s) in the close vicinity acting as possible ligand (first cationic coordination sphere) [16].

In order to scrutinize Fe active sites structure(s) of Fe–ZSM-5, sensitive techniques are requested. One of the most suitable is the interaction of NO probe molecule with the zeolite followed by IR spectroscopy. Besides high sensitivity, this technique could also help to depict the active site structure from biological models, if the similarity of results is demonstrated. For instance, NO interactions on iron porphyrinato complexes Fe(Porph) are involved in vasodilation and neurotransmission mechanisms [17–19]. To investigate this particular Fe heme center formed after coordination to various porphyrinato ligands, NO probe molecule is commonly used followed by IR spectroscopic methods [20–23]. In this case, NO stretch frequency (ν_{NO}) is controlled by the geometry of the Fe–N–O linkage, which can be bent or linear depending on the electronic configuration. According to Enemark and Feltham nomenclature [24], the electron counting formalism and states of Fe–N–O group can be described as $\{FeNO\}^n$ where n corresponds to the number of d electrons on the Fe center plus the unpaired electron from NO. Typically, Fe sites in contact with NO are expected to display a bent Fe–N–O geometry if the iron is in the ferrous state Fe(II). In this case, NO can accept an electron from iron(II) by forming the resonance structure $Fe^{3+}(NO)^-$, since NO^- is isoelectronic with O_2. At contrast, the ferric NO complexes adopt a linear iron-ligand orientation by donating an electron to the iron $d\pi$ orbitals and forming $Fe^{2+}(NO^+)$

---

* Corresponding author. Present address: Laboratoire Catalyse et Spectrochimie, ENSICAEN, Université de Caen, CNRS, 6 Bd Maréchal Juin, F-14050 Caen, France.
E-mail address: mickael.rivallan@ensicaen.fr (M. Rivallan).

0920-5861/$ – see front matter © 2010 Elsevier B.V. All rights reserved.
doi:10.1016/j.cattod.2010.04.014

Table 1
Spectroscopic and electronic characteristics of $\{FeNO\}^n$ groups in Fe(Porph) complexes.

	$\{FeNO\}^6$	NO_g	$\{FeNO\}^7$
ν_{NO} (cm^{-1})	1890–1860	1875	1680–1650
Fe–N–O angle	Linear ~175°	–	Bent ~145°
Resonance form	Fe^{2+} (NO^+)	–	Fe^{3+} (NO^-)
N–O bond (Å)	1.13–1.14	1.154	1.12

Table 2
Fe–ZSM-5 catalysts composition, thermal treatment and activity.

Catalysts	Fe (ppm)	Si/Al	T (K)	Time	Active Fe (%)
$FeZ_{1200}{}^{50}$	1200	50	1273	30 min	20 ± 2
$FeZ_{1200}{}^{120}$	1200	120	1273	30 min	26 ± 2
$FeZ_{2000}{}^{55}$	2000	55	1273	30 min	15 ± 2
$FeZ_{2000}{}^{225}$	2000	225	1273	30 min	0
$FeZ_{2300}{}^{42}$	2300	42	1273	30 min	26 ± 2
$FeZ_{2300}{}^{42}$ (1273 K)	2300	42	1273	15 h	16 ± 2
$FeZ_{2300}{}^{42}$ (973 K)	2300	42	973	30 min	4 ± 2
$FeZ_{2300}{}^{42}$ (823 K)	2300	42	823	30 min	0

resonance form, which is isoelectronic with CO. More in details, for metallo-porphyrins the formation of nitrogen oxides and especially NO_2, have also to be considered because it can then operate as a potential ligand on Fe center as described by Yoshimura for Fe(Porph)(NO)(NO_2) complex [25]. This compound adopts a linear structure $\{FeNO\}^6$ after the reaction of NO (present in excess in the gas phase) forming Fe(Porph)(NO) corresponding to $\{FeNO\}^7$ with a bent structure. This phenomenon is clearly evidenced by infrared spectroscopy where the band due to ν_{NO} stretching frequency at ca. 1890 cm^{-1} vanishes in concomitant appearance of a band at ca. 1670 cm^{-1}, corresponding from linear to bent Fe–N–O group change, respectively. From the extended range of results reported in literature for porphyrinatoiron complexes in interaction with nitric oxide [20–23], the general structure and spectroscopic characteristics observed for $\{FeNO\}^6$ and $\{FeNO\}^7$ complexes are listed in Table 1.

Numerous papers also report the use of NO as probe molecule to titrate iron speciation generated onto Fe–ZSM-5 activated by severe thermal treatment ($T > 1273$ K) [16,26–35]. In this case, Fe^{2+}(NO) mono-nitrosyl species typically absorbs in the 1900–1850 cm^{-1} range, close to ν_{NO} frequencies observed for linear $\{FeNO\}^6$ complex in biology. In a recent review, Zecchina et al. [16] reported strong similarities between $Fe^{2+}(NO)_n$ species adsorbed on mononuclear Fe centers implanted on ZSM-5 and $[Fe(H_2O)_5(NO)]^{2+}$ complex on the basis of UV–vis and IR spectroscopic results. The present paper will focus on *operando* IR spectroscopy of NO interaction and the catalytic reactivity of Fe-containing zeolite to analyze similarities between homogeneous Fe(Porph) complexes, and ferro-nitrosyl species encountered on Fe–ZSM-5. The analogies of both Fe^{2+} centers in contact with NO, the evolution in adsorption and following desorption mechanisms will be the core of the study. Through the similarity observed, the results obtained are discussed shedding some light on the determination of the “alpha” sites structure present on Fe–ZSM-5.

2. Experimental

Fe–ZSM-5 were prepared by hydrothermal synthesis as described elsewhere [29]. Typically, tetraethylorthosilicate (TEOS, Fluka, 98%) was added to an aqueous solution of tetrapropylammonium hydroxide (TPAOH, Fluka, 20% in water) used as a template, $NaAlO_2$ (Riedel-de Haën, Na_2O, 40–45%; Al_2O_3, 50–56%), and $Fe(NO_3)_3{\cdot}9H_2O$ (Fluka, 98%). The molar ratios between components were TEOS:TPAOH:$NaAlO_2$:H_2O = 0.8:0.1:0.016–0.032:33 and Si:Fe = 160:3200. The mixture was stirred for 3 h at room temperature, and the final transparent gel was transferred to a stainless-steel autoclave lined with Teflon and kept in an oven at 450 K for 2 days. The product was filtered, washed with deionized water, and calcined in air at 823 K for 12 h. The zeolite was then converted into the H form by an exchange with a NH_4NO_3 aqueous solution (0.5 M). The samples as prepared are not active and to induce activity the samples were treated in a flow of He at $T = 1273$ K. For comparison, treatments at 823 K and 973 K were also carried out. The chemical composition of the catalysts (Fe and Si/Al ratio) was determined by atomic absorption spectroscopy (AAS) via a Shimadzu AA-6650 spectrophotometer. The samples were dissolved in hot aqua regia containing several drops of HF. The results Fe content and Si/Al ratio are presented in Table 2. The catalysts are referred as $Fe_x{}^y$ where x and y represent Fe content (in ppm) and Si/Al ratio, respectively.

Determination of the total amount of Fe sites in the prepared catalysts active toward N_2O decomposition has been performed via transient response method using a Micromeritics AutoChem 2910 analyzer. After thermal activation, Fe-zeolites have been then cooled down to 523 K in He and a mixture of 2 vol.% N_2O + 2 vol.% Ar + 96 vol.% He (20 ml min^{-1}) was introduced for 10 min. This leads to the deposition of atomic “alpha” oxygen on vacant active Fe sites $(\ )_\alpha$ following the equation:

$$N_2O + Fe(\ )_\alpha \rightarrow Fe(O)_\alpha + N_2 \tag{1}$$

After the purge by He, the temperature programmed desorption of oxygen is performed with a ramp at 20 K min^{-1} under inert flow (20 ml min^{-1}). At ca. 700–750 K, “alpha” oxygen recombination and desorption occur:

$$2Fe(O)_\alpha \rightarrow O_2 + 2Fe(\ )_\alpha \tag{2}$$

Based on the stoichiometry of the previous reaction, this technique (O_2-TPD) is able to give a reasonable estimation of active Fe sites population (2 active Fe sites for each O_2 mole desorbed). In the present paper dealing with nitric oxide adsorption/desorption mechanisms on active sites, the O_2-TPD titration has been considered rather than classical N_2O decomposition or CO oxidation (by $(O)_\alpha$) transient responses, because the data obtained in O_2 recombination are expected to be closer to the real active sites population. In fact the catalytic reactions involved in the two others techniques (oxidation or reduction, respectively) may also occur on inactive iron sites (clusters) and catalytic products (NO_x) could be also formed, thus leading to some discrepancies and overestimation of active species concentration.

Temperature programmed desorption of nitric oxide (NO-TPD) has been monitored by mass spectrometry after previous NO adsorption on fresh activated catalysts (~0.5 g_{cat}) at room temperature for 7 min interaction (0.5 vol.% NO in He at a constant flow rate of 20 ml min^{-1}). During the increase of temperature from RT to 873 K at a ramp of 30 K min^{-1} under inert flow (He at 20 ml min^{-1}), the following amu (m/e) have been collected: 18 (H_2O), 28 (N_2), 30 (NO), 32 (O_2), 40 (Ar), 44 (N_2O), 46 (NO_2) in order to determine the amount of reactant and/or catalysis products adsorbed and their respective temperature of desorption and/or decomposition.

The IR spectra were collected on a PerkinElmer 2000 FTIR instrument equipped with a cryogenic MCT detector and running at 4 cm^{-1} resolution. The samples were in the form of self-supporting pellets (ca. 25 mg) and placed into titanium IR flow through reactor cell sealed with CaF_2 windows suitable for measurements in transmission mode. The temperature of the sample was monitored by a thermocouple (K) placed in the core of the IR cell allowing *in situ* treatment from room temperature (RT) until 773 K. The whole assembly was connected to a gas manifold system for providing precise flow of gases (NO and He) regulated by mass flow controllers. The Fe–ZSM-5 catalysts have been pre-treated at 773 K for

30 min in He at a flow rate of 50 ml min^{-1} in order to clean the surface of the catalysts and then directly cooled down in same gas mixture. Afterwards a reference spectrum was collected at RT in the 4000–1500 cm^{-1} fingerprint of the catalyst before nitric oxide contact. This background spectrum is then subtracted to the next spectra in order to monitor adsorption, catalytic reaction(s) and/or desorption dynamic(s) during sample exposition to subsequent 1.0 vol.% NO at a constant flow rate of 100 ml min^{-1} in He. In order to get quantitative comparison between the different samples, the displayed spectra have been normalized as function of the thickness of the pellet, i.e. the absorption of the framework overtones of the reference spectrum in the 2000–1500 cm^{-1}.

3. Results and discussion

3.1. NO probe on Fe–ZSM-5 followed by FTIR

IR spectra of Fe–ZSM-5 in interaction with NO and following purge by He at RT are displayed in Fig. 1a and b. The influences of treatment conditions (temperature and time) and active Fe sites concentration (Table 2) have been investigated.

From the diverse IR spectra shown in Fig. 1a, whatever the activation treatment previously performed (temperature and time), all the samples in contact with NO display two broad bands centered at 1610 and 1580 cm^{-1}, stable at RT upon evacuation in He. It may be related to NO_2 and/or NO_3 groups strongly adsorbed on defects of the MFI framework (silanols) or Fe clusters [31,36,37].

At higher wavenumbers, an extended band centered at ca. 1860 cm^{-1} appears on $FeZ_{2300}{}^{42}$ sample activated at 823 K. This band also evidenced after deconvolution (dotted lines) on activated samples, is quite controversial and has been tentatively related to $Fe^{II}O_x$–NO complex [38]. Increasing the temperature of activation pre-treatment until 1273 K (and following interaction with NO at RT), leads to the appearance of two others components at 1877 and 1890 cm^{-1} (shoulder). These two bands are commonly observed on Fe-zeolites in interaction with nitric oxide in dynamic conditions (IR flow through reactor) and are assigned to mono-nitrosyl species bonds onto Fe^{2+} centers: $FeAlO_x$ and Fe^{2+} in (α) or (γ) positions, respectively [30,31,37].

From Fig. 1c and d, it can be noticed that these two bands are linearly proportional to the active Fe content determined from O_2-TPD, after ZSM-5 loading by atomic oxygen from N_2O (Table 2). This observation is quite contentious, because when *in situ* conditions are used (NO titration in static, activation under vacuum), the bands due to poly-nitrosyl adsorption are additionally observed and found to be proportional to the activity. In the present study dealing with operando measurement, only mono-nitrosyl species emerge, and as a consequence they will be attributed to the active Fe species in N_2O decomposition [29,30,37]. From this last point and Fig. 1c, it can be so concluded that $T > 1000$ K is requested to form active Fe species from isomorphously substituted ZSM-5.

After 25 min purge by He, the mono-nitrosyl species in the 1925–1825 cm^{-1} upper range totally disappear (Fig. 1a and b). In response, two new bands centered at 1635 and 1625 cm^{-1} (sh), greatly grow up. Other groups observe the same equilibrium between the bands at 1877 and 1635 cm^{-1} upon flowing of He or O_2 during NO evacuation [30,39–41]. After isotopic labeled titration (with ^{15}NO; blue shift of ca. 35 cm^{-1}) the band at 1635 cm^{-1} has been assigned to nitro NO_2 group, probably adsorbed on $FeAlO_x$ species [39,40]. More in details, the intensities of the bands at 1890 and 1877 cm^{-1} observed under NO gas phase follow the same trend and seem also to be proportional (1:1) to the bands observed at 1625 and 1635 cm^{-1}, respectively (upon purging under inert gas). It is also important to note that under *in situ* conditions of measurement (vide infra), this doublet at 1890 and 1877 cm^{-1} cannot be removed from Fe sites at such low temperature range [37,42]. These observations may suggest that the disappearance of these two bands concomitant with appearing of 1635 and 1625 cm^{-1} is due to a reorganization of nitrosyl species. A possible explanation could be a change in symmetry of Fe–N–O group passing from linear NO^+ to bent NO^-. This mechanism will be detailed in the following part.

3.2. Stability of linear nitrosyl under NO gas phase

Even if the comparison between Fe sites formed on Fe–ZSM-5 and those of homogeneous models is not straightforward, it is quite reasonable to notice some surprising similarities toward nitric oxide interaction at room temperature (RT). In the case of evaluation, Yoshimura's complex (nitro)(nitrosyl)iron(II) porphyrinates [25], could be the most appropriate homogeneous complex because of its controversial existence. The formation of such complex $Fe(Porph)(NO)(NO_2)$ $\{FeNO\}^6$ has been first described as being the result of Fe(Porph)(NO) $\{FeNO\}^7$ in excess of NO, after previous disproportionation phenomena leading to nitro $NO_2{}^-$ group formation and stabilization onto Fe heme center (Fig. 2a) [25].

Recently, this proposal has been totally revised by Lorkovic et al. using carefully de-aerated solutions and purified NO [43]. They only characterized mono-nitrosyl Fe(Porph)(NO) complex at RT (and also dinitrosyl at low temperature). From these considerations it has been so concluded that the formation of the nitro group in Yoshimura's complex: $Fe(Porph)(NO)(NO_2)$, incomes from O_2/NO_2 presence (impurities) [44]. This first observation is quite adequate with what is observed for Fe–ZSM-5 in excess of gaseous NO and following evacuation in He [37] or O_2 [30]. Under these conditions (Fig. 1a and b), IR bands due to mono-nitrosyl at 1890 and 1877 cm^{-1} vanish and as a result two other components at 1635 and 1625 cm^{-1} grow up. In the case of He evacuation, the presence of O_2/NO_2 traces may come from gases used (difficult to control in operando conditions), or the result of the NO interaction on active vacant $Fe^{2+}(\ )_\alpha$ sites. It could be also due to oxygen atoms adsorbed on the samples during previous calcinations' treatment [37]. This is also the case reported in biology for the reaction of NO in excess with μ-oxo dimer $[Fe(Porph)]_2O$ (Fig. 2b) which leads to the eventual formation of $Fe(Porph)(NO)(NO_2)$ complex [45] (Notice that in such case, isonitrosyl (–O) and side-on (–NO) linkage isomers could also be observed). Nevertheless, for Fe-zeolites, the oxygen adsorption/deposition from O_2 on Fe sites is not directly possible, besides, previous alpha oxygen deposition (from N_2O) is generally done to achieve an isotopic exchange (with ^{18}O) on such active Fe centers.

Whatever is the genesis of O_2/NO_2 molecule interacting with Fe-zeolites, the most important point concerns the equilibrium between the IR bands centered at 1890–1877 and 1635–1625 cm^{-1} (Fig. 1c and d). They are the same as reported for Fe(Porph) with respective bands at ca. 1890 and 1670 cm^{-1} due to linear $\{FeNO\}^6$ and bent $\{FeNO\}^7$ complexes. In both case, the linear Fe–N–O group is stable only under NO atmosphere. Thus, if NO excess is removed, the reaction turns back to the right side of the equilibrium (Fig. 2b) and bent $\{FeNO\}^7$ group is recovered. In the case of homogeneous model, this is correlated to the removal of nitro group (adsorbed on the picket side) which gives the linearity to the N–O bond onto complex (on the open porphyrin face).

3.3. Reversibility between linear and bent nitrosyl

The equilibrium between $\{FeNO\}^6$ and $\{FeNO\}^7$ is also surprisingly reversible [25]. In fact, upon introducing new excess of NO, IR band centered at $\nu_{NO} = 1890$ cm^{-1} characteristic of $Fe(Porph)(NO)(NO_2)$ complex is recovered and the IR band at ca. 1670 cm^{-1} wholly vanishes. The analogous reversibility is

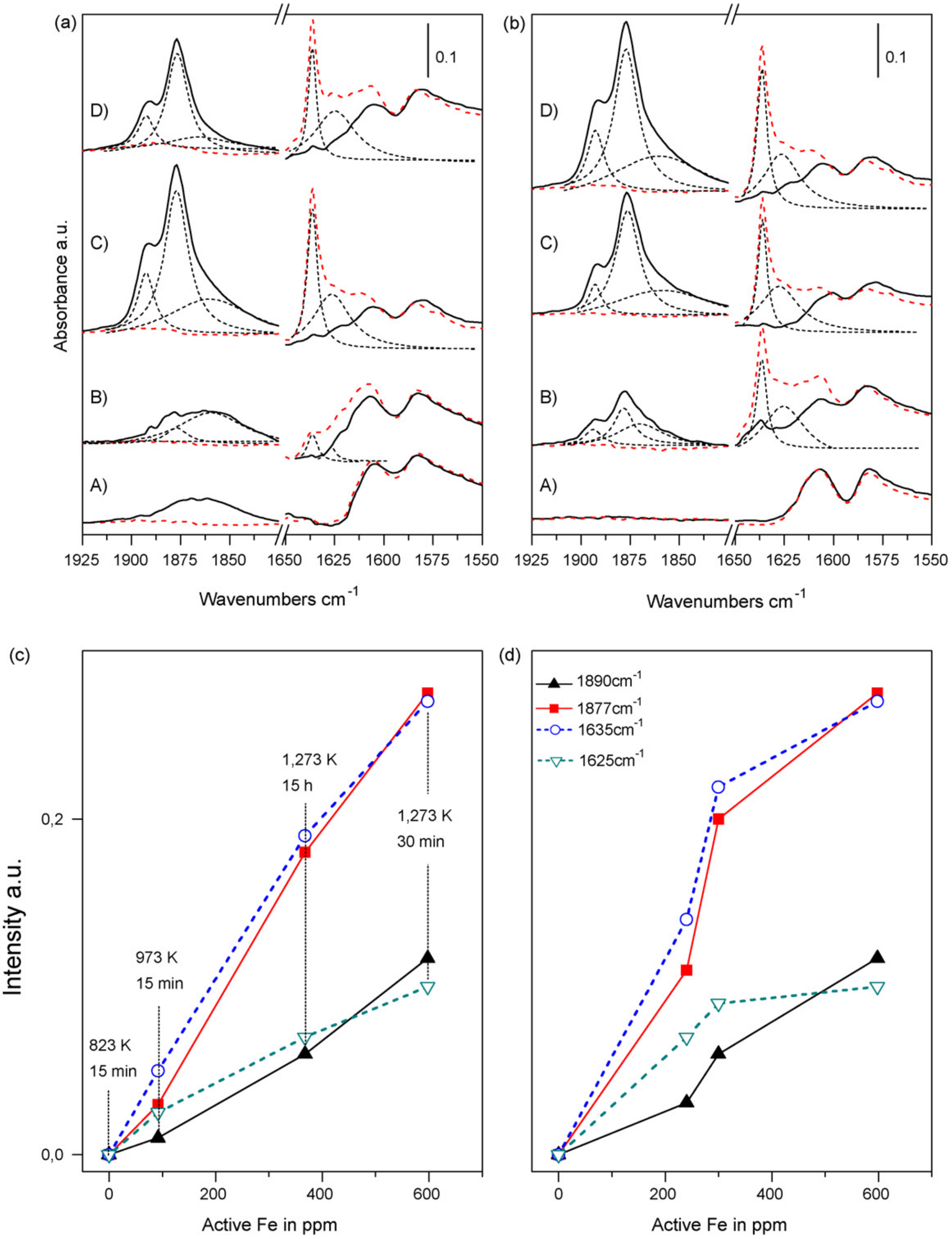

Fig. 1. Relation between activity and mono-nitrosyl species adsorbed on Fe centers of ZSM-5. (a) Spectra of adsorbed NO (solid lines) and following purge by He (dashed lines) at RT on $FeZ_{2300}{}^{42}$ activated at 1273 K for 15 h (D) or 30 min (C) and at 973 K (B), 823 K (A) for 30 min; (b) on $FeZ_{2300}{}^{42}$ (D); $FeZ_{2000}{}^{55}$ (C); $FeZ_{1200}{}^{50}$ (B); $FeZ_{2000}{}^{225}$ (A), respectively. (c) Intensities of the IR bands centered at 1890–1877 cm^{-1} under NO gas phase (solid lines) and 1635–1625 cm^{-1} under He purge (dotted lines) as function of active iron for $FeZ_{2300}{}^{42}$ activated at different temperatures; (d) for $FeZ_{2300}{}^{42}$, $FeZ_{2000}{}^{55}$, $FeZ_{1200}{}^{50}$ and $FeZ_{2000}{}^{225}$ activated at 1273 K for 30 min.

observed for Fe–ZSM-5 when coming back to nitric oxide gas phase (Fig. 3a) on previously NO-evacuated catalyst (at RT) [30].

Such reversibility may testify that the IR bands at 1635/1625 cm^{-1} cannot be assigned to a nitrito group, because it is quite difficult to conceive a mechanism leading to the recovery of nitrosyl species from previous adsorbed nitrito or nitro group (and its substitution again more, even if NO is a reducing agent). The previous nitro assignment from isotopic label becomes also indecisive, if we consider Fe(Porph)(NO) isotopically substituted by ^{15}NO [25]. In this case the ν_{NO} frequency is blue shifted of ca. 35 cm^{-1} as reported for supposed $^{15}NO_2$ adsorbed on supposed $Fe^{II}AlO_x$ species [30]. Moreover, we may remark in Fig. 1c and d that the absorbance intensities due to the species in the upper range (1890 and 1877 cm^{-1}) are close to those observed at lower frequency (1635 and 1625 cm^{-1}). These same extinction coefficients could indicate transition between similar nitrogen oxides species (i.e. nitrosyl).

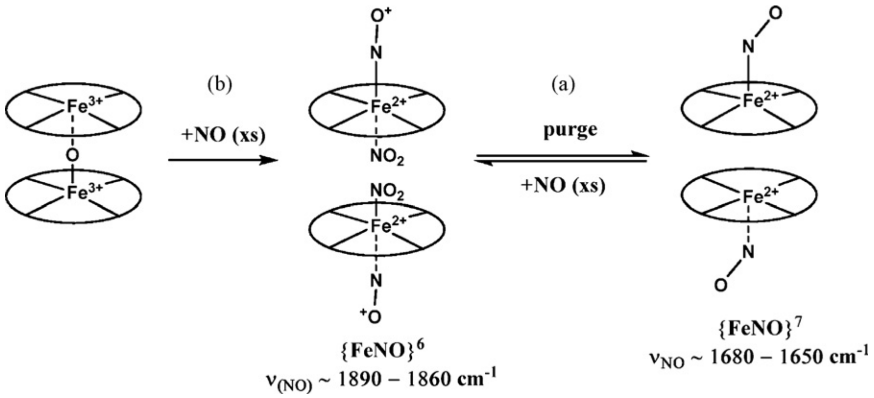

Fig. 2. Nitric oxide reactions on Fe-porphyrins. (a) Equilibrium between Fe(Porph)(NO) and Fe(Porph)(NO)(NO_2) with bent and linear nitrosyl, respectively and (b) monomerisation of $[Fe(Porph)]_2O$ after NO reactions on oxobridge.

Stretching frequencies ν_{NO} of linear and bent Fe–N–O groups depend on $d\pi$ back-bonding ability of the Fe^{2+} mononuclear center, i.e. of ligands coordination. This observation reported on porphyrinatoiron(II) is also suitable for Fe^{2+} centers present into Fe–ZSM-5. As a result the two IR bands displayed at 1890 (sh) and 1877 cm^{-1} in presence of NO and assigned to linear Fe–N–O are certainly due to the presence of two Fe^{2+} sites which are different in their ligand coordinations. Coming back to dimer $[Fe(Porph)]_2O$ model which originates two identical Fe(Porph) after NO contact [45], the same mechanisms can be supposed for Fe–ZSM-5, i.e. the initial species (binuclear) may originate into two Fe sites which are different in their respective environment and are consequently acting differently in adsorption of NO with bands at 1890 and 1877 cm^{-1}. This shift in frequency could be assumed as due to

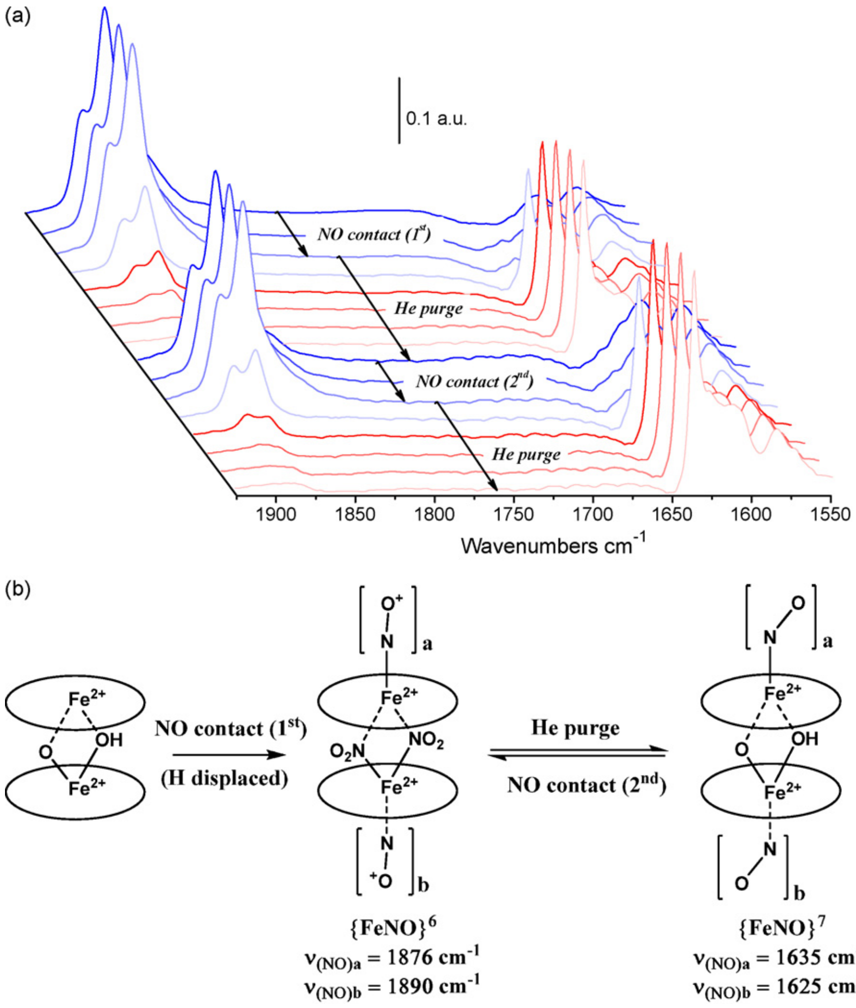

Fig. 3. Reversibility between linear and bent Fe–N–O groups. (a) Spectra of adsorbed NO on $FeZ_{2300}{}^{42}$ at RT first dose for 5, 10 and 15 min; and following evacuation for 5, 10, 15, 20 and 25 min; then direct second dose for 5, 10 and 15 min; and following evacuation for 5, 10, 15, 20 and 25 min. (b) Mechanisms of NO adsorption and desorption observed for dinuclear active site structure of Fe–ZSM-5, on the basis of iron porphyrins biological models.

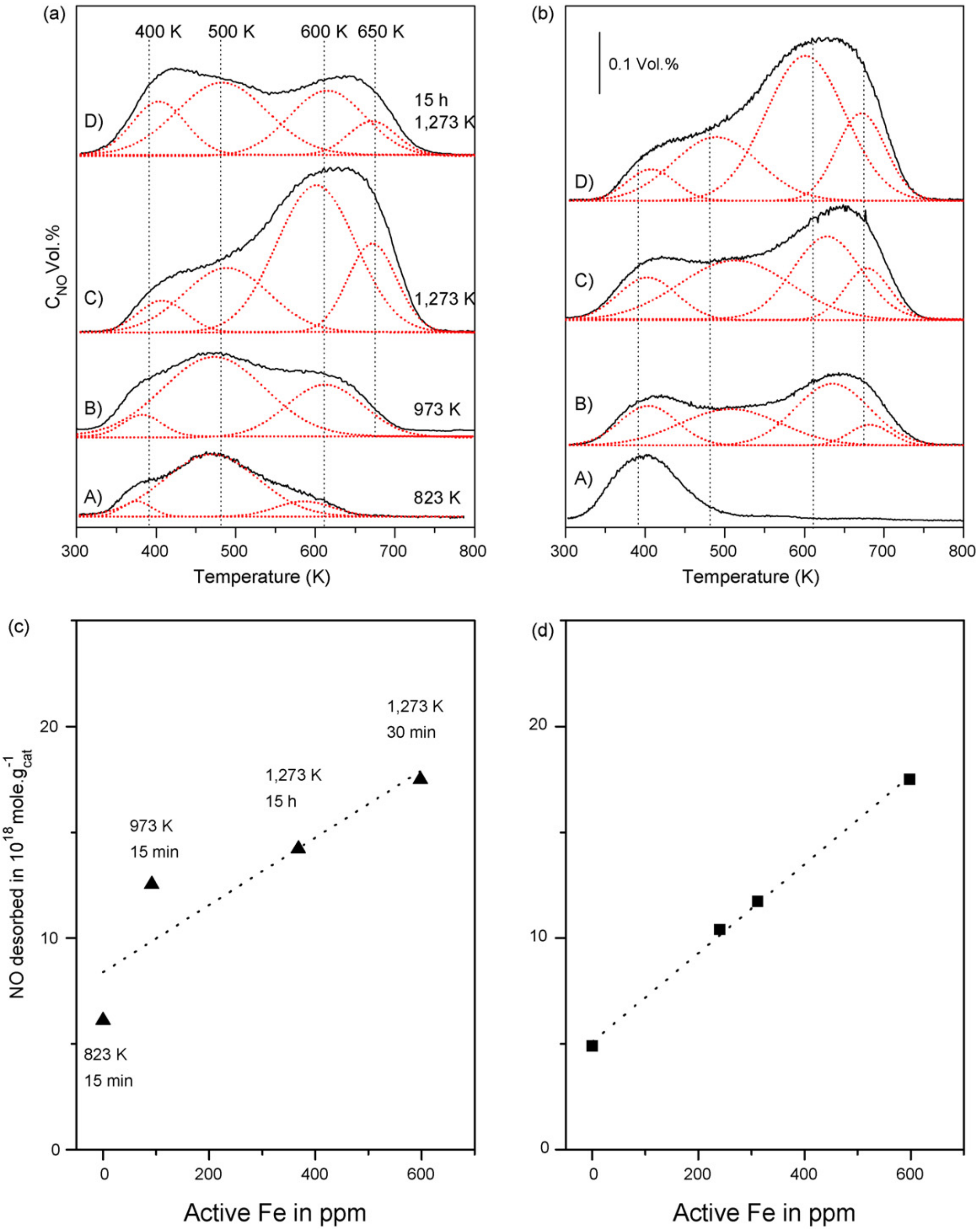

Fig. 4. Relation between activity and NO desorption. NO-TPD profiles (a and b), of $FeZ_{2300}{}^{42}$ activated for 30 min at 823 K (A), 973 K (B), 1273 K (C) and for 15 h at 1273 K (D) (a); and of $FeZ_{2000}{}^{225}$ (A); $FeZ_{1200}{}^{50}$ (B); $FeZ_{2000}{}^{55}$ (C) and $FeZ_{2300}{}^{42}$ (D) activated at 1273 for 30 min and contacted in NO for 7 min at RT (b). Total NO desorbed (in 10^{18} mol g_{cat}^{-1}) computed from NO-TPD as function of active Fe (in ppm) (c and d), for the same catalyst $FeZ_{2300}{}^{42}$ (c); and for $FeZ_{2300}{}^{42}$, $FeZ_{1200}{}^{120}$, $FeZ_{1200}{}^{50}$ and $FeZ_{2000}{}^{225}$ activated at 1273 K for 30 min (d).

the presence (or not) of an Al atom in the first cationic coordination sphere of Fe atom. As a result, linear or slightly bent Fe–N–O groups may be involved, respectively. The ratio intensities of the IR bands centered at 1877 and 1890 cm^{-1} is constant for the whole set of Fe-zeolites reported here. This means that the ratio between both monomer species is kept from one catalyst to another. On the other hand, this ratio (close to ~2) cannot allow quantitative comparison of the respective populations of the two $Fe^{2+}(NO)$ mono-nitrosyl species for a same sample.

This is, however, an oversimplification of the real zeolitic environment of Fe^{2+} center under NO gas phase. In fact, as reported above for metallo-porphyrins, the reversible equilibrium is due to the bond and release of the nitro group from ferrous center. The formation of such nitro-nitrosyl porphyrin species (six-coordinate system) is possible because the ferrous center proposes two different sides available to nitrosyl and nitro group bounds: on the picket side and on the open porphyrin face. When Fe–ZSM-5 catalysts are concerned, it is also interesting to hypothesize a possible NO_x species adsorbed in the environment of Fe^{2+} centers under NO gas phase. First, because Fe^{2+} sites are supposed to be unsaturated species, and consequently may allow such double adsorption on the same metal atom, and also because several nitrosyl groups are generally observed by IR spectroscopy on the isolated ferrous center in static conditions (vide infra) [32]. It can be probably lodged in between of both iron atoms under NO atmosphere. When gradually purging NO from IR cell, the nitro group may be simply outgassed or dislodged into MFI matrix in the close environment of Fe sites and ready to react again upon coming back to NO gas phase. Such NO_x group is difficult to detect first because classical *in situ* IR cell windows suitable for high temperature condition scarcely transmit below 1000 cm^{-1}, and also intense absorptions due to siliceous MFI matrix also occur in this 1400–1000 cm^{-1} range, where ν_{sym} (strong) of nitro ligand of $Fe(Porph)(NO)(NO_2)$ [46,47] and nitro groups in general [48] are expected to stand, while ν_{asym} (weak) is at ca. 1500 cm^{-1}. However, it has to be noticed that a slight change in absorbance is observed in the 1550–1450 cm^{-1} range upon purging in He (Fig. 1a and b). Sachtler and co-workers also observed absorption at ca. 1300 cm^{-1} when exposing Fe-MFI to NO + O_2 mixture [49–51]. In order to confirm NO/NO_x groups remaining stable under inert gas phase at RT, NO-TPD have been performed.

3.4. Temperature programmed desorption of nitric oxide

Fig. 4a and b displays NO-TPD profiles performed on Fe–ZSM-5 previously contacted for 7 min in NO gas phase, and following purged for 5 min in He at RT. Activation treatment (temperature and time; on left part) and active Fe sites concentration have been investigated.

From NO-TPD profiles obtained, we may first conclude that a substantial quantity of NO physisorbed and/or chemisorbed remained at RT on the surface of activated Fe–ZSM-5 catalysts (activation at $T > 1000$ K). As depicted for inactive $FeZ_{2000}{}^{225}$ (low Al content) and H–ZSM-5, [52] the total NO adsorption area cannot be only due to Fe active sites (low concentration below 2000 ppm), the adsorption on defects sites or inside zeolitic MFI channels have to be considered. Nitrites and nitrates groups are also certainly present and may desorb through decomposition mechanisms. These compounds are unfortunately difficult to discriminate from NO signal. [52].

Two different temperature ranges of NO desorption can be barely distinguished at 400–500 K and 600–650 K. The first desorption in the 400–500 K range appear to be present and constant for the whole set of catalysts studied. However, a significant increase is observed when increasing time of activation at 1273 K. Such severe treatment is supposed to break MFI framework crystallinity. As a consequence it may be correlated to N_2O_3 or physisorbed NO_x [52] on the generated defects or on inactive Fe clusters.

The desorption occurring at ca. 600–650 K is clearly due to active sites because NO desorption area greatly increases as function of temperature of activation, i.e. as function of active sites formation and also notably diminishes with time of activation, i.e. due to deactivation mechanism (15 h at 1273 K). Nevertheless, the nature of this desorbed species remains difficult to assign. The increase observed is certainly due to the progressive formation of unsaturated sites which enhance the possibility of NO uptake. In fact it has been dressed from IR results that active sites may adsorb both NO and NO_x at the same Fe^{2+} center under NO gas phase. But as already discussed previously, NO_x species may already desorb at low temperature upon purging by He, so we would rather consider this last desorption as due to mono-nitrosyl (bent) desorbing from Fe active sites. To confirm this idea, desorption followed by IR spectroscopy have been performed on Fe–ZSM-5 previously contacted with NO at RT (not shown). From the results obtained, it has been found that the bands at 1635–1625 cm^{-1} due to the bent Fe–N–O group, do not persist at $T > 600$ K under He flow [49]. It can be so concluded that the signal observed in NO-TPD at $T > 600$ K corresponds to NO coming from Fe sites. NO-TPD profiles also display two distinct peaks after deconvolution, confirming the presence of two different active Fe centers releasing NO at ca. 600 K and 650 K. Moreover, the area ratio seems to be kept for all active catalysts meaning that both NO desorptions may income from same hosting structure. These observations strongly suggest the presence of dinuclear sites allowing two NO adsorptions on two different Fe^{2+} centers. This situation was also emerging from IR spectra (Fig. 1a and b), where Fe sites differentiate by the presence of Al atom (or not) in the 1st cationic coordination sphere.

To complete the comparison between Fe–ZSM-5 catalysts and porphyrinatoiron(II) complexes reacting with NO, Fig. 3b summarizes the mechanisms of NO adsorption at RT and following desorption on Fe^{2+} centers of dinuclear structure. Adsorption and consecutive desorption mechanisms are dressed. It has to be noted that biological $[Fe(Porph)]_2O$ dimer model with Fe^{3+} centers (Fig. 2b) is only ready to react and adsorb NO after rupture of μ-oxobridge resulting in Fe^{2+} metal charged ions. While for Fe-zeolites it is commonly accepted that Fe^{2+} metal ion is the starting form of the active sites after thermal activation and that rupture mechanism is not necessary for Fe–ZSM-5 and in a certain manner would be also rather difficult to conceive because NO bent/linear transition is reversible. In Fig. 3b, the initial bridge between both Fe^{2+} sites is designed as (μ-O)(μ-OH) binuclear structure, recently reported thermodynamically stable [53]. On this model, NO may adsorb on the bridge but also form Fe–N–O linkage upon NO gas phase (in excess). NO interaction on such bridge may lead into acid nitric HNO_x formation or simply displace hydroxyl group on adjacent positions.

4. Conclusions

Reaction(s) of NO probe molecule has been followed through FTIR spectroscopy to investigate active sites of Fe–ZSM-5 which form “alpha oxygen” from N_2O known as highly active in selective benzene oxidation to phenol. Upon flowing NO gas phase through IR cell, Fe sites adsorbed one NO molecule leading to the formation of $Fe^{2+}(NO)$ species with $\nu_{NO} = 1890–1877$ cm^{-1}. When gradually purging NO (by He), IR bands due to mono-nitrosyl species totally vanished in respect to the formation of two new components centered at $\nu_{NO} = 1635–1625$ cm^{-1}. This equilibrium is found to be reversible upon coming back to NO atmosphere and also surprisingly similar to phenomena observed for iron porphyrins complexes in interaction with NO. For instance, $Fe(Porph)(NO)(NO_2)$ Yoshimura’s biological model exhibits the same reversible equilibrium with Fe(Porph)(NO). In this case, the transition is claimed as due to changes of metal–ligand orientation, passing from linear to bent Fe^{2+}–N–O linkage with $\nu_{NO} = 1890–1675$ cm^{-1}, respectively upon reducing NO concentration. In the present paper, the same biological concept is adapted to active Fe center in Fe–ZSM-5 catalysts. From the comparison and analogies dressed, the two IR bands observed for Fe–ZSM-5 at $\nu_{NO} = 1635–1625$ cm^{-1} upon purging NO, are assigned to bent nitrosyl groups on Fe^{2+} active sites, leading to $Fe^{2+}(NO^+)$ resonance form. The two different bands also imply two different iron sites differing from their ligand coordination, where the presence (or not) of Al atom is supposed to be responsible.

Further in analogies with biochemistry, and after consideration of the $[Fe(Porph)]_2O$ dimer model as second potential originating species of Yoshimura’s complex under NO, a dinuclear $[Fe^{2+}$(μ-O)(μ-OH)$Fe^{2+}]$ structure is also proposed for Fe–ZSM-5 active site. This structure is in good agreement with experiment because mono-nitrosyl duplicity is observed for Fe^{2+} active sites (from

FTIR spectroscopy); and also the ratio populations between both Fe^{2+}(NO) species remains constant for the whole set of catalysts under the study. Similarly to the nitro group found in Fe(Porph)(NO)(NO_2) biological model, the formation of a NO_2 molecule after NO interaction onto the bridge of dinuclear Fe site of ZSM-5 is also strongly suggested. This species is capable to substitute μ-hydroxobridge (reversible upon evacuation).

Acknowledgements

Financial supports of SNSF and EU NoE IDECAT are acknowledged.

References

[1] G.I. Panov, G.A. Sheveleva, A.S. Kharitonov, V.N. Romannikov, L.A. Vostrikova, Applied Catalysis A—General 82 (1992) 31.
[2] G.D. Pirngruber, P.K. Roy, R. Prins, Physical Chemistry Chemical Physics 8 (2006) 3939.
[3] G.I. Panov, V.I. Sobolev, K.A. Dubkov, A.S. Kharitonov, 11th International Congress on Catalysis—40th Anniversary, Pts A and B, vol. 101, 1996, p. 493.
[4] H.A. Xia, K.Q. Sun, K.J. Sun, Z.C. Feng, W.X. Li, C. Li, Journal of Physical Chemistry C 112 (2008) 9001.
[5] N. Hansen, A. Heyden, A.T. Bell, F.J. Keil, Journal of Physical Chemistry C 111 (2007) 2092.
[6] K.A. Dubkov, N.S. Ovanesyan, A.A. Shteinman, E.V. Starokon, G.I. Panov, Journal of Catalysis 207 (2002) 341.
[7] L. Kiwi-Minsker, D.A. Bulushev, A. Renken, Journal of Catalysis 219 (2003) 273.
[8] A.A. Battiston, J.H. Bitter, D.C. Koningsberger, Journal of Catalysis 218 (2003) 163.
[9] P. Marturano, L. Drozdova, A. Kogelbauer, R. Prins, Journal of Catalysis 192 (2000) 236.
[10] Y. Shiota, K. Suzuki, K. Yoshizawa, Organometallics 25 (2006) 3118.
[11] G. Centi, S. Perathoner, F. Pino, R. Arrigo, G. Giordano, A. Katovic, V. Pedula, Catalysis Today 110 (2005) 211.
[12] J.A. Ryder, A.K. Chakraborty, A.T. Bell, Journal of Catalysis 220 (2003) 84.
[13] N.A. Kachurovskaya, G.M. Zhidomirov, E.J.M. Hensen, R.A. van Santen, Catalysis Letters 86 (2003) 25.
[14] K. Yoshizawa, T. Yumura, Y. Shiota, T. Yamabe, Bulletin of the Chemical Society of Japan 73 (2000) 29.
[15] M. Rivallan, G. Ricchiardi, S. Bordiga, A. Zecchina, Journal of Catalysis 264 (2009) 104.
[16] A. Zecchina, M. Rivallan, G. Berlier, C. Lamberti, G. Ricchiardi, Physical Chemistry Chemical Physics 9 (2007) 3483.
[17] A.R. Butler, D.L.H. Williams, Chemical Society Reviews 22 (1993) 233.
[18] M. Hoshino, L. Laverman, P.C. Ford, Coordination Chemistry Reviews 187 (1999) 75.
[19] D.A. Wink, J.B. Mitchell, Free Radical Biology and Medicine 25 (1998) 434.
[20] P.C. Ford, I.M. Lorkovic, Chemical Reviews 102 (2002) 993.
[21] T.S. Kurtikyan, P.C. Ford, Coordination Chemistry Reviews 252 (2008) 1486.
[22] M.D. Lim, I.M. Lorkovic, P.C. Ford, Journal of Inorganic Biochemistry 99 (2005) 151.
[23] G.R.A. Wyllie, W.R. Scheidt, Chemical Reviews 102 (2002) 1067.
[24] J.H. Enemark, R.D. Feltham, Coordination Chemistry Reviews 13 (1974) 339.
[25] T. Yoshimura, Inorganica Chimica Acta 83 (1984) 17.
[26] G. Berlier, C. Prestipino, M. Rivallan, S. Bordiga, C. Lamberti, A. Zecchina, Journal of Physical Chemistry B 109 (2005).
[27] G. Berlier, G. Spoto, G. Ricchiardi, S. Bordiga, C. Lamberti, A. Zecchina, Journal of Molecular Catalysis A—Chemical 182 (2002) 359.
[28] G. Berlier, A. Zecchina, G. Spoto, G. Ricchiardi, S. Bordiga, C. Lamberti, Journal of Catalysis 215 (2003) 264.
[29] I. Yuranov, D.A. Bulushev, A. Renken, L. Kiwi-Minsker, Applied Catalysis A—General 319 (2007) 128.
[30] G. Mul, J. Perez-Ramirez, F. Kapteijn, J.A. Moulijn, Catalysis Letters 80 (2002) 129.
[31] L.J. Lobree, I.C. Hwang, J.A. Reimer, A.T. Bell, Journal of Catalysis 186 (1999) 242.
[32] G. Spoto, A. Zecchina, G. Berlier, S. Bordiga, M.G. Clerici, L. Basini, Journal of Molecular Catalysis A—Chemical 158 (2000) 107.
[33] K.I. Hadjiivanov, Catalysis Reviews—Science and Engineering 42 (2000) 71.
[34] M. Rivallan, G. Berlier, G. Ricchiardi, A. Zecchina, Studies in Surface Science and Catalysis 170B (2007) 1357.
[35] G. Berlier, C. Lamberti, M. Rivallan, G. Mul, Physical Chemistry Chemical Physics 12 (2010) 358.
[36] K. Hadjiivanov, Catalysis Letters 68 (2000) 157.
[37] K. Sun, H. Xia, Z. Feng, R. van Santen, E. Hensen, C. Li, Journal of Catalysis 254 (2008) 383.
[38] M. Lezcano, V.I. Kovalchuk, J.L. d'Itri, Kinetics and Catalysis 42 (2001) 104.
[39] T. Nobukawa, K. Sugawara, K. Okumura, K. Tomishige, K. Kunimori, Applied Catalysis B—Environmental 70 (2007) 342.
[40] E.M. El-Malki, R.A. van Santen, W.M.H. Sachtler, Journal of Catalysis 196 (2000) 212.
[41] H.Y. Chen, T. Voskoboinikov, W.M.H. Sachtler, Journal of Catalysis 180 (1998) 171.
[42] R. Kefirov, E. Ivanova, K. Hadjiivanov, S. Dzwigaj, M. Che, Catalysis Letters 125 (2008) 209.
[43] M.D. Lim, I.M. Lorkovic, P.C. Ford, Nitric Oxide, Pt E, Vol. 396, Elsevier Academic Press Inc, San Diego, 2005, p. 3.
[44] M. Wolak, R. van Eldik, Coordination Chemistry Reviews 230 (2002) 263.
[45] M.F. Settin, J.C. Fanning, Inorganic Chemistry 27 (1988) 1431.
[46] T.S. Kurtikyan, A.A. Hovhannisyan, M.E. Hakobyan, J.C. Patterson, A. Iretskii, P.C. Ford, Journal of the American Chemical Society 129 (2007) 3576.
[47] I.V. Novozhilova, P. Coppens, J. Lee, G.B. Richter-Addo, K.A. Bagley, Journal of the American Chemical Society 128 (2006) 2093.
[48] K. Nakamoto, Infrared and Raman Spectra of Inorganic and Coordination Compounds, Wiley and Sons, New York, 1970.
[49] H.Y. Chen, E.M. El-Malki, X. Wang, R.A. van Santen, W.M.H. Sachtler, Journal of Molecular Catalysis A—Chemical 162 (2000) 159.
[50] K. Hadjiivanov, H. Knozinger, B. Tsyntsarski, L. Dimitrov, Catalysis Letters 62 (1999) 35.
[51] Z.X. Gao, S. Qi, W.M.H. Sachtler, Applied Catalysis B—Environmental 33 (2001) 9.
[52] R.Q. Long, R.T. Yang, Journal of Catalysis 198 (2001) 20.
[53] H. Guesmi, D. Berthomieu, L. Kiwi-Minsker, Journal of Physical Chemistry C 112 (2008) 20319.